

NAVAL ENVIRONMENTAL PREDICTION RESEARCH FACILITY MON--ETC F/G 4/2
METEOROLOGICAL FACTORS AFFECTING EVAPORATION DUCT HEIGHT CLIMAT--ETC(U)
JUL 80 W SWEET
NEPRF-TR-80-02 NL

NL

1 OF 2
AD A
09-66

~~END
OF
FILED
12-80
BTIC~~

CONT.



LEVEL

12

NAVENVPREDRSCHFAC
TECHNICAL REPORT
TR 80-02

NAVENVPREDRSCHFAC TR 80-02

METEOROLOGICAL FACTORS AFFECTING EVAPORATION DUCT HEIGHT CLIMATOLOGIES

Wayne Sweet

Naval Environmental Prediction Research Facility

AD A091665

JULY 1980

DTIC
SELECTED
NOV 18 1980

DDC FILE COPY



APPROVED FOR PUBLIC RELEASE
DISTRIBUTION UNLIMITED

80 11 10 052

NAVAL ENVIRONMENTAL PREDICTION RESEARCH FACILITY
MONTEREY, CALIFORNIA 93940

QUALIFIED REQUESTORS MAY OBTAIN ADDITIONAL COPIES
FROM THE DEFENSE TECHNICAL INFORMATION CENTER.
ALL OTHERS SHOULD APPLY TO THE NATIONAL TECHNICAL
INFORMATION SERVICE.

UNCLASSIFIED

SECURITY CLASSIFICATION OF THIS PAGE (When Data Entered)

REPORT DOCUMENTATION PAGE		READ INSTRUCTIONS BEFORE COMPLETING FORM
1. REPORT NUMBER NAVENVPREDRSCHFAC Technical Report TR 80-02	2. GOVT ACCESSION NO. AD-A097665	3. RECIPIENT'S CATALOG NUMBER
4. TITLE (and Subtitle) Meteorological Factors Affecting Evaporation Duct Height Climatologies		5. TYPE OF REPORT & PERIOD COVERED Final Rpt.
7. AUTHOR(s) Wayne/Sweet		6. PERFORMING ORG. REPORT NUMBER
9. PERFORMING ORGANIZATION NAME AND ADDRESS Naval Environmental Prediction Research Facility Monterey, CA 93940		10. PROGRAM ELEMENT, PROJECT, TASK AREA & WORK UNIT NUMBERS PE 62759N NEPRF WU 6.2-11
11. CONTROLLING OFFICE NAME AND ADDRESS Naval Ocean Systems Center San Diego, CA 92152		12. REPORT DATE July 1980
14. MONITORING AGENCY NAME & ADDRESS (if different from Controlling Office) Naval Air Systems Command Department of the Navy Washington, DC 20361		13. NUMBER OF PAGES 28
		15. SECURITY CLASS. (of this report) UNCLASSIFIED
16. DISTRIBUTION STATEMENT (of this Report) Approved for public release; distribution unlimited.		15a. DECLASSIFICATION/DOWNGRADING SCHEDULE
17. DISTRIBUTION STATEMENT (of the abstract entered in Block 20, if different from Report)		
18. SUPPLEMENTARY NOTES		
19. KEY WORDS (Continue on reverse side if necessary and identify by block number) Evaporation duct Duct climatology		
20. ABSTRACT (Continue on reverse side if necessary and identify by block number) Latitudinal and seasonal variations of calculated evaporation duct height climatologies are examined to determine which of the four surface-measured input parameters to the calculation of duct height -- air temperature, sea surface temperature, dew point temperature, and wind speed -- has the largest effect on the climatological tendencies. Based on a sensitivity analysis of the four parameters, sea surface temperature appears to cause most of the latitudinal variation. -- (continued on reverse)		

DD FORM 1473

1 JAN 73

EDITION OF 1 NOV 65 IS OBSOLETE
S/N 0102-014-6601

UNCLASSIFIED

SECURITY CLASSIFICATION OF THIS PAGE (When Data Entered)

704271

UNCLASSIFIED

SECURITY CLASSIFICATION OF THIS PAGE(When Data Entered)

Block 20, ABSTRACT, Continued

Seasonal variations of median duct height apparently are caused by the stability (indicated by the difference between air and sea surface temperatures) and dew point temperature, and, to a lesser extent, by wind speed.

UNCLASSIFIED

SECURITY CLASSIFICATION OF THIS PAGE(When Data Entered)

CONTENTS

1. INTRODUCTION	1
2. EVAPORATION DUCT HEIGHT CALCULATION	3
3. LATITUDINAL AND SEASONAL VARIATIONS	7
4. EFFECTS OF SURFACE-MEASURED PARAMETERS ON CALCULATION OF EVAPORATION DUCT HEIGHT	11
4.1 Introduction	11
4.2 Air-Sea Temperature	14
4.3 Wind Speed	17
5. CLIMATOLOGICAL CAUSES OF LATITUDINAL AND SEASONAL VARIATIONS OF MEDIAN DUCT HEIGHTS	19
6. SUMMARY.	25
References	26
Distribution: pp 27-33	

Accession For	
NTIS GRA&I	<input checked="checked" type="checkbox"/>
DTIC TAB	<input type="checkbox"/>
Unannounced	<input type="checkbox"/>
Justification	
By _____	
Distribution/	
Availability Codes	
Dist	Special
A	

1. INTRODUCTION

Evaporation ducts affect the propagation of many surface-to-surface radars currently used by the Fleet. Duct height is the factor that determines which radar will be affected. Duct height is computer-calculated from observations of four surface-measured input parameters: air temperature, sea surface temperature, dew point temperature, and wind speed.

This report relates latitudinal and seasonal variations of calculated median heights of evaporation ducts to climatological variations of the input parameters, for ten ocean weather stations in the North Atlantic.* The range of latitudinal and seasonal variations of the median duct height contains the "crucial duct height values" for many naval radars (defined and described in NOSC, 1978). These crucial duct heights are considered to separate radar ranges into two classes: normal and extended.

An understanding of the general effects of climatic parameters on evaporation duct heights is important to fleet meteorologists who must assess and forecast refractive conditions. In regions where no evaporation duct climatologies have been developed (e.g., most of the Southern Hemisphere's oceans), climatological values of the four input parameters can give useful information about the expected behavior of evaporation duct heights; and thus can aid in the development of better assessment and forecasting techniques.

*A climatology of evaporation duct occurrence at these stations is given in Sweet (1979); see references.

This report discusses the evaporation duct phenomenon and describes the process for determining duct height. Values of the input parameters are varied in order to determine the effects of such variations on the resulting calculations of duct height. Latitudinal and seasonal variations are explained in terms of the primary input parameters.

2. EVAPORATION DUCT HEIGHT CALCULATION

Evaporation over oceanic regions causes strong negative vertical water vapor gradients, (i.e., water vapor rapidly decreasing with height) normally within 30 meters (m) of the surface. These water vapor gradients in turn produce gradients in refractivity which are large enough to cause microwave ducts to form with tops generally up to 30 m above the surface.

The determination of duct height from temperature and water vapor profiles is not operationally practical because it is very hard to measure these parameters with the necessary resolution. Parametric techniques have been developed, however, to use four surface-measured parameters -- air temperature, relative humidity, wind speed, and sea-surface temperature -- as input to a complex set of equations (run on a programmable calculator) to determine duct height.

Inherent errors, due to measuring-instrument errors, in the scheme used to calculate duct height were examined in NAFI, 1977. Worst case situations were evaluated and large errors in the calculated duct heights were noted: 100-200% errors in some cases. Typical cases, however, would probably reveal errors only between 10% and 25%. Such shortcomings can not be considered a serious factor in climatological compilations developed from many years of data for two reasons: first, because instrument errors tend to cancel out over many years of data; and second, because few observations will be worst case combinations of all four instrument errors.

Measurement data from the ten North Atlantic ocean weather stations (OWS) shown in Figure 1 -- archived by the National Climatic Center, Asheville, NC, for the period 1949 to 1970 -- were used for this present study. These data form the most complete set available encompassing a major area within a specific oceanic region. Over all stations, data were missing only for about 10% of the observations; these breaks in continuity presumably occurred because of operational problems and/or errors in data processing. (The one exception is OWS Hotel, which was decommissioned in the 1960's and later reestablished in the early 1970's for nine months of each year.)

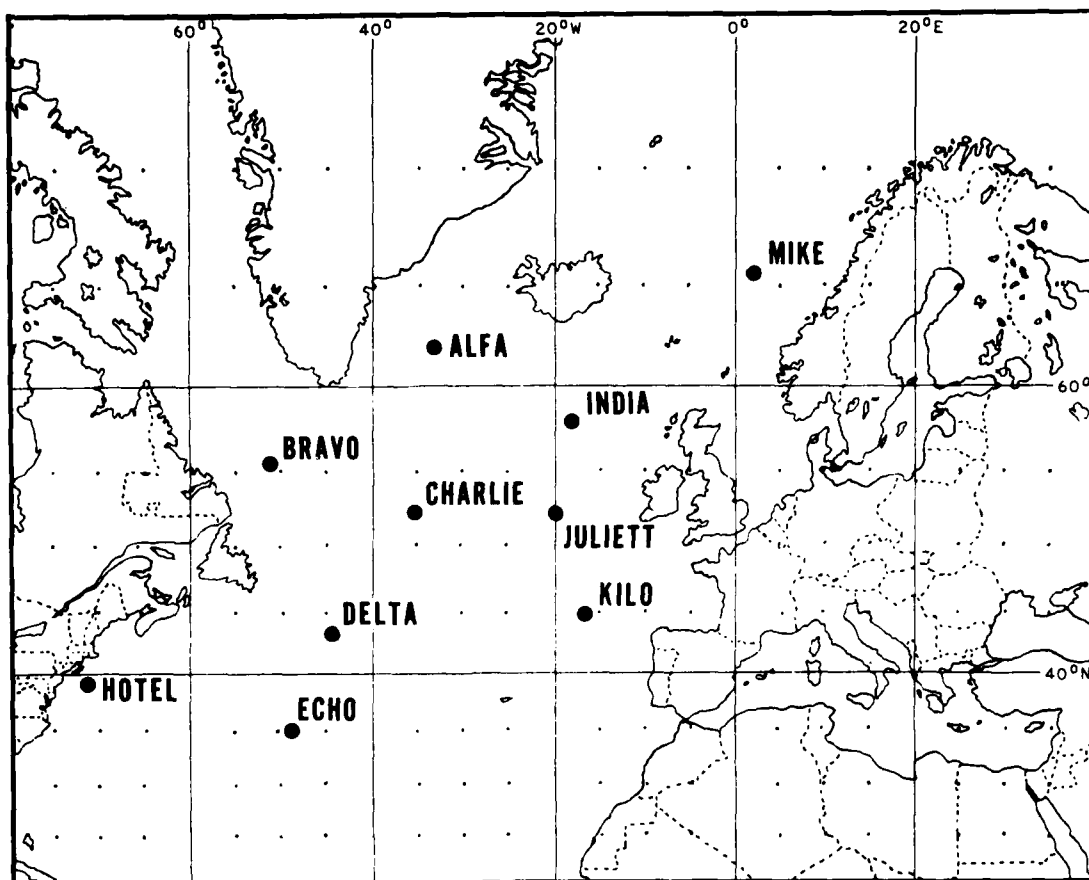


Figure 1. Locations of ocean weather stations (OWS) in the North Atlantic Ocean that provided data for the present study.

<u>Station</u>	<u>Location</u>	<u>Station</u>	<u>Location</u>
ALFA	62°N, 33°W	HOTEL	36°N, 70°W
BRAVO	56°N, 51°W	INDIA	58°N, 19°W
CHARLIE	52°N, 35°W	JULIETT	52°N, 20°W
DELTA	44°N, 41°W	KILO	45°N, 18°W
ECHO	35°N, 48°W	MIKE	66°N, 2°E

3. LATITUDINAL AND SEASONAL VARIATIONS

Evaporation duct heights vary with latitude; heights generally increase as latitudes decrease, a trend that is observed in all of this present study's central tendency statistics (monthly means, modes, and medians). The exceptions are OWS ALFA and BRAVO, and to some degree CHARLIE, which show smaller medians than other stations near their latitude. Figure 2 shows this variation of duct height with latitude. Note, the variation is less pronounced, and indeed not clearly supported by Figure 2, at the higher latitudes. (This high latitude disagreement will be discussed later.) Table 1 shows monthly medians of evaporation duct heights for the ten stations in order of descending latitudes.

Seasonal variations of median duct heights show a minimum during the summer and a maximum during the fall. A variation of more than 3 m in the average median duct height for the ten stations is shown in Figure 3a. The extremely large data sample size makes this variation statistically significant.

The months of maximum and minimum monthly median duct heights vary depending on the station, but overall the minimum heights occur during the period May-July and the maximum heights occur from September to December. The spread between the maximum and minimum monthly median duct heights also shows a latitudinal variation, with larger spreads occurring in the lower latitudes, as depicted in Figure 3b. The stations with the smaller minimum values show the larger of the spreads for stations located at similar latitudes.

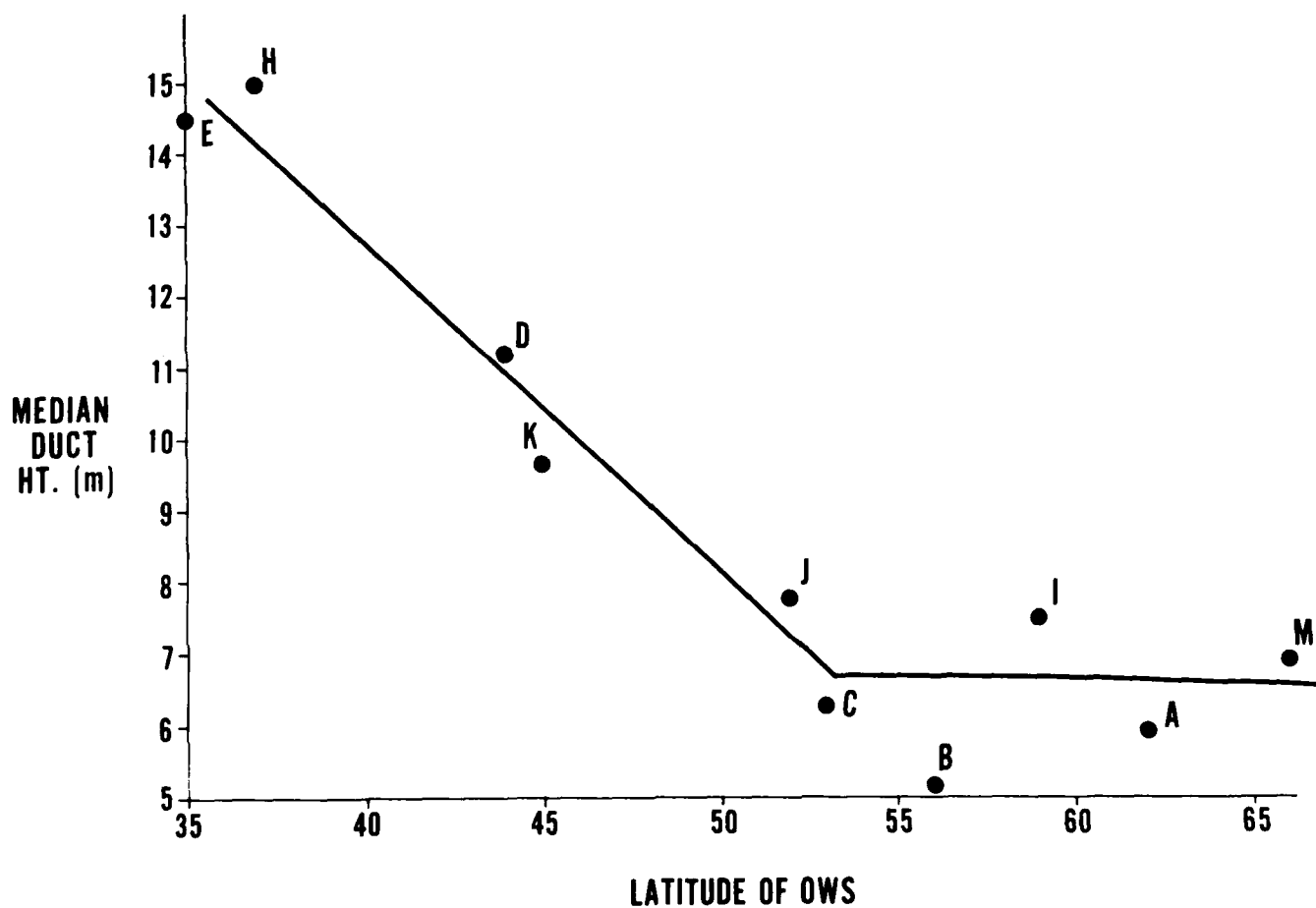


Figure 2. Plot of median duct heights versus latitude, showing the general decrease of heights with increasing latitudes. Median annual duct height is the height exceeded half of the time during the year.

Table 1. Median duct heights for each ocean weather station for each month. Average station median and average monthly median are given along the left and bottom margins, respectively.

Average (OWS)	JAN	FEB	MAR	APR	MAY	JUN	JUL	AUG	SEP	OCT	NOV	DEC	OWS
6.8	7.3	7.4	7.1	6.5	6.2	6.0	6.0	6.5	6.9	7.1	7.3	7.5	MIKE 66°N
5.9	6.4	6.3	6.1	5.7	5.0	4.5	4.8	5.7	6.7	6.7	6.5	6.9	ALFA 62°N
7.5	7.6	7.6	7.8	7.6	7.6	6.7	6.4	7.0	7.5	7.8	7.9	8.1	INDIA 59°N
5.1	5.5	5.1	5.3	5.0	4.1	3.5	2.6	4.1	6.5	6.9	6.1	6.1	BRAVO 56°N
6.1	7.0	6.5	6.2	5.6	5.0	4.2	3.5	5.4	7.2	7.8	7.3	7.4	CHARLIE 53°N
7.8	8.2	8.5	7.1	7.4	7.6	6.3	6.9	7.9	7.9	8.3	8.9	8.3	JULIETT 52°N
9.6	8.9	9.9	8.2	8.8	8.0	8.0	9.6	10.8	11.1	11.4	11.6	9.0	KILO 45°N
11.3	13.2	12.6	11.7	10.5	9.3	7.0	7.6	10.6	13.0	13.4	13.4	13.0	DELTA 44°N
15.1	14.1	14.2	14.0	14.9	13.7	12.7	13.8	15.7	17.9	17.5	16.5	15.8	HOTEL 37°N
14.4	14.8	14.0	14.2	12.0	10.7	11.2	14.7	16.8	17.1	16.2	16.3	15.0	ECHO 35°N
Monthly Average	9.3	9.2	8.8	8.4	7.7	7.0	7.6	9.0	10.2	10.3	10.2	9.7	--

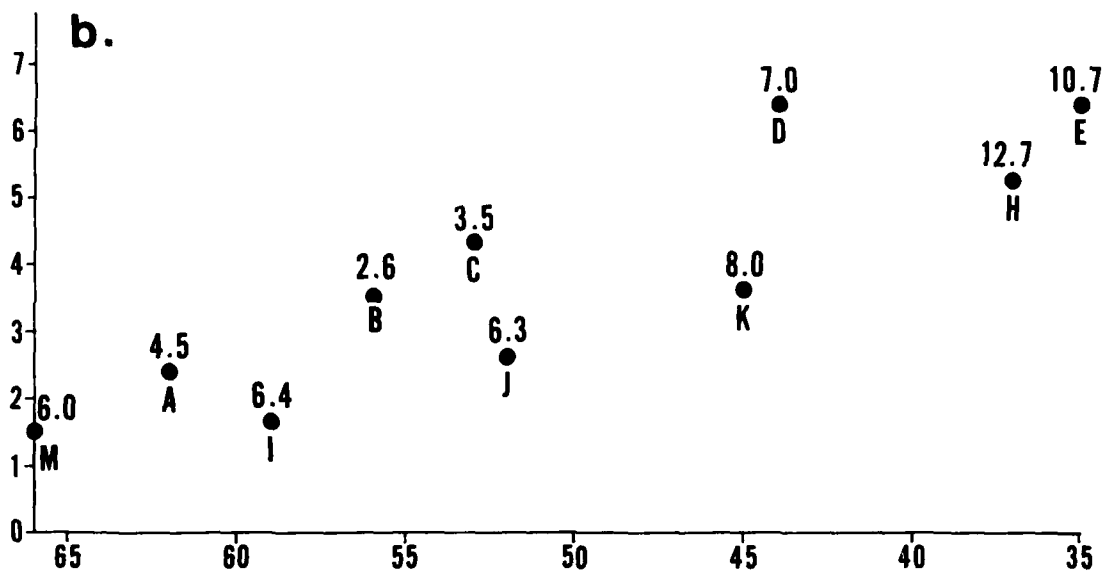
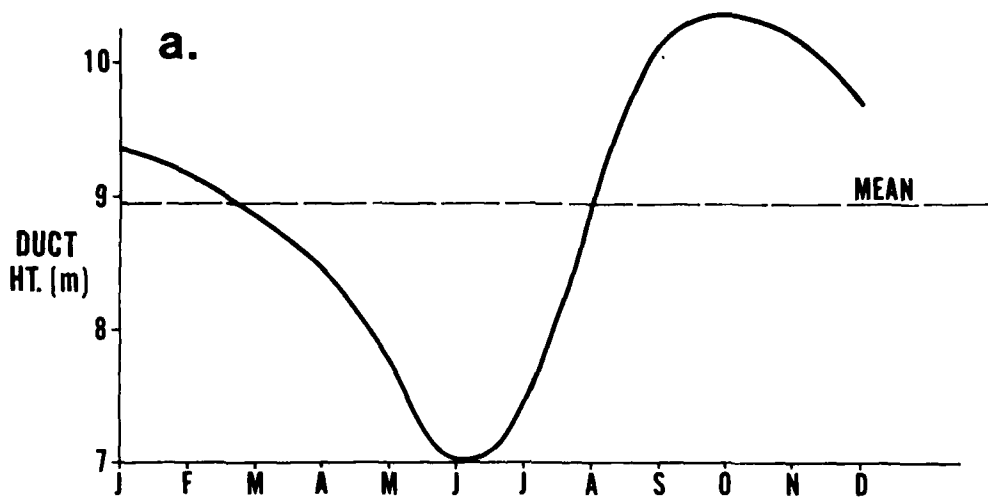


Figure 3. (a) Monthly medians of duct heights for all OWS. (b) Plot of duct height differences between maximum and minimum monthly medians. The number at each OWS plot is the minimum monthly median duct height at that station.

4. EFFECTS OF SURFACE-MEASURED PARAMETERS ON CALCULATION OF EVAPORATION DUCT HEIGHT

4.1 INTRODUCTION

The surface-measured parameters used as input to the calculation* of evaporation duct height (represented below by D) are air temperature (TA), sea surface temperature (TS), dew point temperature (TD), and wind speed (U).

Since dew point temperature (TD) can be calculated from air temperature (TA) and relative humidity (RH), and the difference between air and sea surface temperatures (hereafter represented by AS) has the physical significance of stability (h), the four parameters above can also be represented by the combination TS , RH , AS , and U .

Examination of the relationship of duct height (D) to variations in the input parameters requires some understanding of the functional dependence of D . A closed form expression of D does not exist; the equations used to find D depend in general on stability h and the vertical gradient of refractivity. This vertical gradient, ΔN , in turn, is represented by the difference in refractivity at the observation height, usually 10 meters, and at the surface, $\Delta N = N - N_s$. Using h to indicate the stability factor, then

$$D = D(h, \Delta N).$$

The stability factor is closely related to the shape of the N profile. According to boundary layer theory (Gossard, 1978),

*Accomplished by using set of equations described in Hitney, 1975.

for neutral stability the N profile in the first few decameters (i.e., about 100 ft) has a logarithmic shape (i.e., very rapidly decreasing with height) near the surface with a gradual transition to a linear shape above (i.e., less rapidly decreasing). For slightly stable conditions the profile becomes nearly linear throughout, with only a small region (about 2-3 m) near the surface having a logarithmic curved tail. The unstable region is represented by a profile similar to the neutral case, but with a sharper curved section near the surface.

Figure 4 illustrates these three stability conditions. The numbered short horizontal lines indicate the relative duct heights for the three profiles; number 1 is unstable, 2 is neutral, and 3 is stable. These duct heights are determined by the slope of the profile; specifically, where the slope exceeds the value -157 N/km . Stable conditions allow higher duct heights since mixing from dry air aloft is at a minimum. Neutral and unstable conditions allow progressively more mixing from above, thereby suppressing the steep gradients to progressively lower levels.

Consideration of just the stability factor would lead one to expect the duct height to increase as the stability increases. Figure 5 is a plot of stability ($1/L$, L is the Monin-Obukhov length*) versus duct height showing such a relationship. The curves are drawn for several values of ΔN , where

$$\Delta N = N (\text{observation ht}) - N (\text{surface})$$

* L is a measure of stability that accounts for both convective mixing due to air-sea temperature differences and mechanical mixing due to wind.

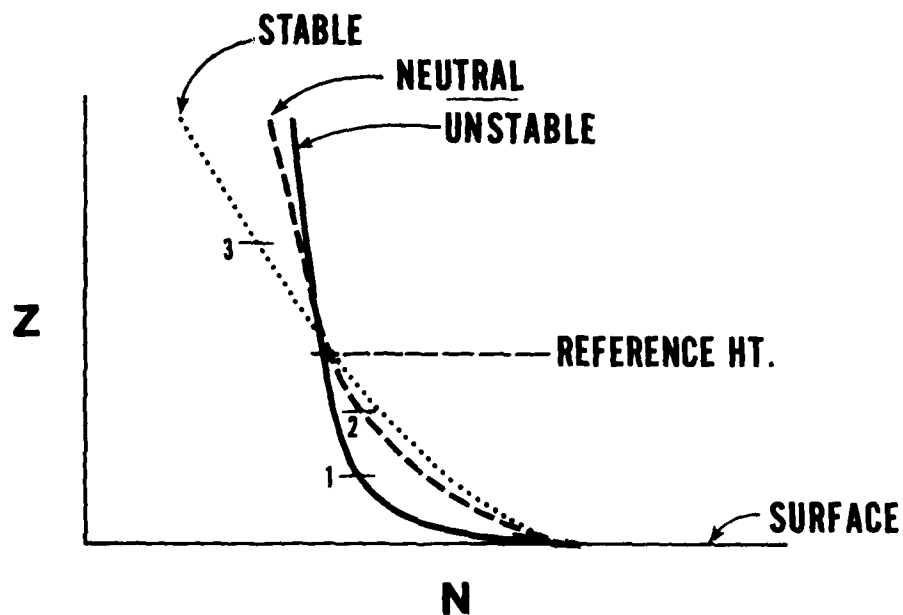


Figure 4. Three stability conditions as indicated by N profiles.

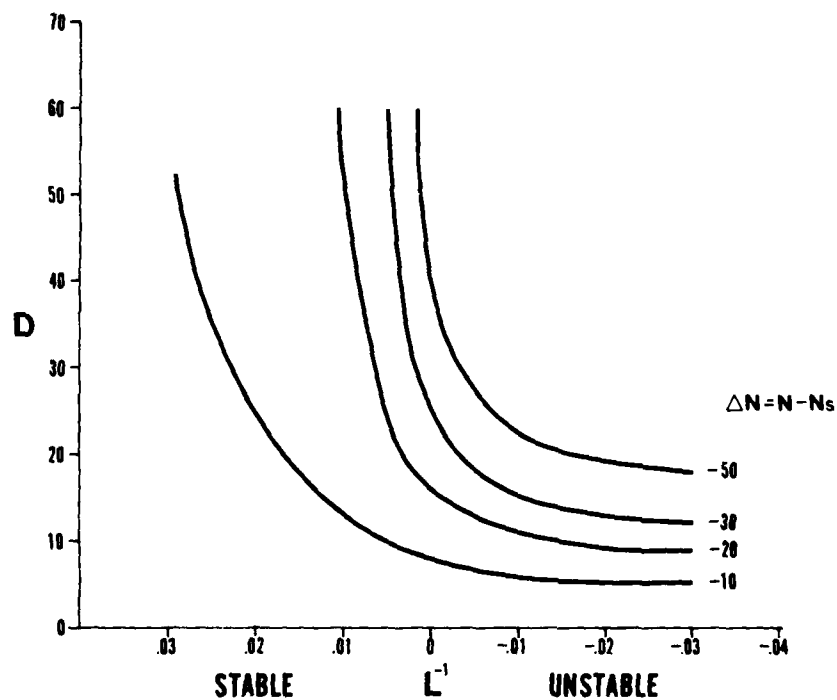


Figure 5. Plot of relationship of stability factor to duct height.

Large absolute values of ΔN lead to higher ducts. As ΔN becomes larger in absolute value, the curves change slope sharply after crossing into the stable region ($L^{-1} > 0$). This rapid change in slope of the ΔN curves will be important in later discussions.

4.2 AIR-SEA TEMPERATURE

The relationship of duct height to stability is not easily interpreted in terms of the four observed input parameters, TS, TA, TD, and U, because L is a combination of both air-sea temperature difference and wind speed. Plotting duct height versus air-sea temperature difference, AS (equal to TA-TS) for various TD and U values allows direct climatological application. Four curves of duct height versus AS for various TD and U values are shown in Figure 6, a graph that reveals some unexpected characteristics.

The variation of duct height with AS shows a general increase with decreasing convective stability. The dashed curves are for a higher wind speed (30 kt) (i.e., more mechanical mixing) and show this general increase with decreasing AS. The solid curve (i.e., 15 kt wind) with the lower humidity (TD=16), however, shows a hump in the slightly stable region which the other three curves do not.

This hump can be explained by reference to Figure 7. Dashed curves (a) and (b) represent the solid curves (a) and (b) respectively in Figure 6. The hump is a result of the stability L^{-1} dominating the values of duct height near the neutral region, for the lower RH values. In the following explanation, TA is held constant, so as AS decreases, TS increases and hence $\Delta N = N - N_s$

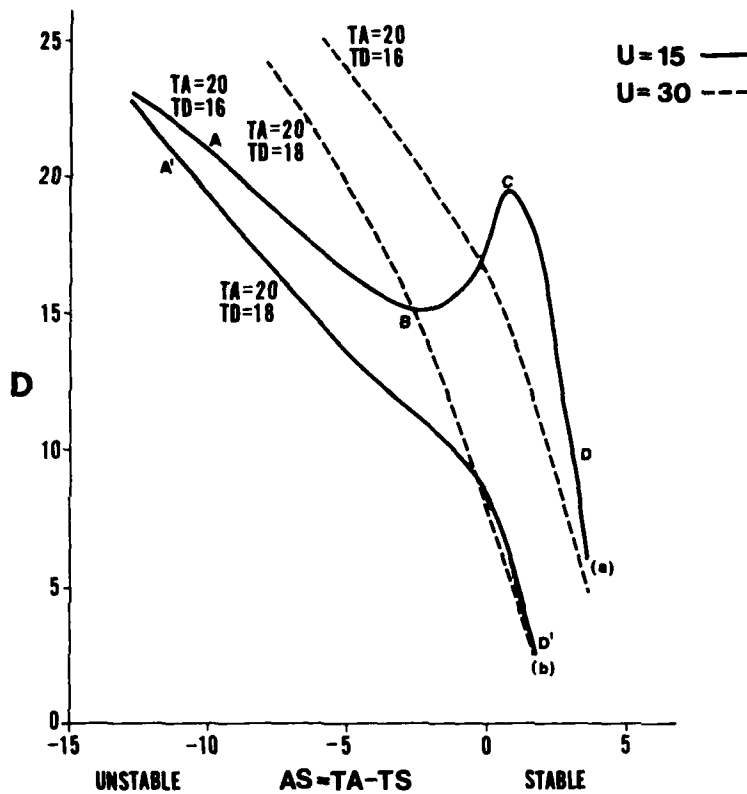


Figure 6. Plot of duct height versus $AS (=TA-TS)$ for various values of TD (dew point temperature) and TA (air temperature).

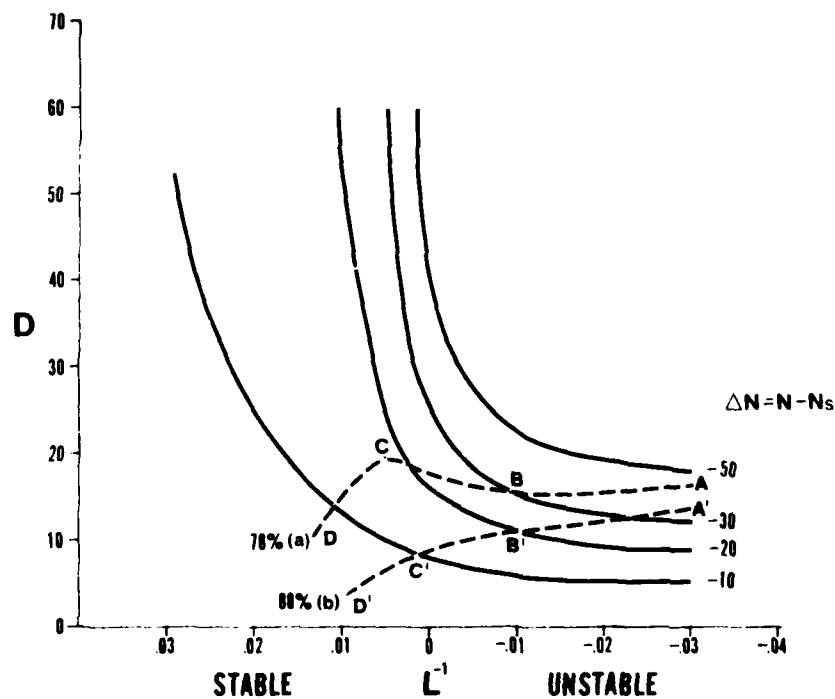


Figure 7. Neutral conditions require L^{-1} to be equal to 0; compare with Figure 6.

becomes more negative. Duct heights generally increase for the stronger ΔN gradients, other factors being held constant.

Consider first curve (a) in Figure 7. Compared to point D, point C has a larger TS value (for constant TA), a stronger ΔN gradient (more negative) and hence a much larger duct height (D) value. This larger D value results from the rapidly changing form (slope) of the various ΔN curves in the near neutral region. Point B however has a lower D value than point C since the change in ΔN , as AS and TS increase, is more than offset by the steep slope of the ΔN curves on the slightly unstable side of neutral. Therefore the duct height decreases in the region between C and D (see Figure 6). Point A has a larger D value than point B simply because the flatness of the D versus L^{-1} allows the changing value of ΔN (as AS decreases) to force D to higher values. In comparison to curve (a), curve (b) in Figure 7 (and Figure 6) has lower values of ΔN due to the higher RH value. Curve (b) therefore remains in the region of the D versus L^{-1} family of curves which all have gradual slopes. Therefore ΔN is the dominant factor throughout the variation of AS; as a result, in Figure 6 D increases steadily from D' to A'.

For higher wind speeds (U) the mechanical mixing forces the stability L^{-1} more toward neutral, and the changing AS (and hence TS) values result from ΔN being the determining factor in duct height.

4.3 WIND SPEED

Increasing wind speeds cause increasing duct heights if sea surface temperatures are higher than the air temperatures (unstable), and decreasing duct heights if sea surface temperatures are lower than the air temperatures (stable). Figure 8 illustrates these trends for two values of TS. Increasing winds drive the stability toward neutral due to the increase in mechanical mixing. From Figure 7 it is clear that Figure 8 is correct since ΔN does not change value and the lowest of points for varying wind simply follow the given ΔN curve.

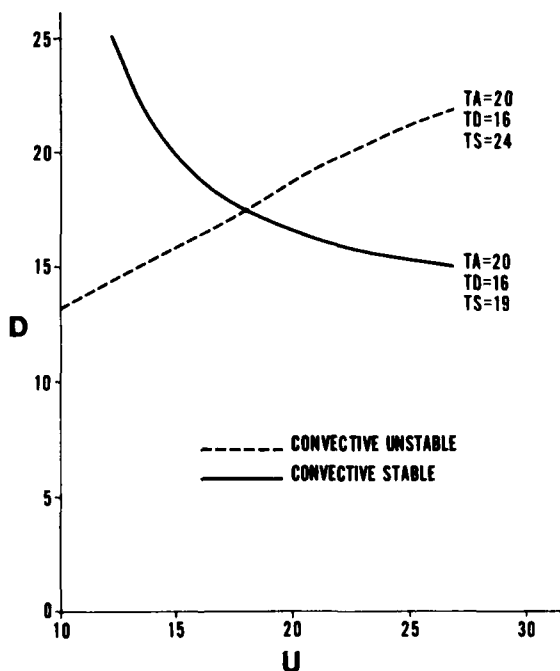


Figure 8. Variations in duct height (D) at increasing wind speeds (U) for values of air temperature (TA), dew point temperature (TD) and sea surface temperature (TS).

The preceding conclusions can be summarized for application to climatological data by realizing that sea surface temperatures force the value of air temperatures. Higher sea surface temperatures cause higher air temperatures and higher dew point temperatures. If the relative humidities and winds are in the range $RH < 85\%$ and $U < 25$ kt, respectively, then high ducts can result for sea surface temperatures slightly less than the air temperatures, (i.e., in the "hump" region of Figure 6). To summarize in tabular format,

	AS>0 Stable	AS<0 Unstable
TD	$D \propto \frac{1}{TD}$	$D \propto \frac{1}{TD}$
TS	$\begin{cases} D \propto TS \\ D \propto \frac{1}{TS}^* \end{cases}$	$D \propto TS$
U	$D \propto \frac{1}{U}$	$D \propto U$

*See above text.

5. CLIMATOLOGICAL CAUSES OF LATITUDINAL AND SEASONAL VARIATIONS OF MEDIAN DUCT HEIGHTS

The inverse relationship between latitude and duct height was noted in Section 3. Based on the discussion in Section 4, the cause for this increasing duct height as latitudes decrease is apparently due to the higher TS and the resulting higher TA values at the lower latitudes. Figures 9 and 10 show isopleths of TS in the North Atlantic, and median duct heights at each of the 10 ocean weather station locations, for the months of November and June, respectively. The relationships of duct heights to TS values are certainly not perfect, but they are clearly apparent. The slight exceptions to the latitudinal relationship are stations INDIA, MIKE and JULIETT; these three are in regions of predominantly warm ocean currents, and thus would be expected to have slightly higher duct heights.

The primary causes of seasonal variations are air-sea temperature differences, and wind speed and dew point temperature differences, between the maximum and minimum duct height seasons. The minimum median duct height occurs during the warm months when stability is nearly neutral or slightly stable, and the dew point temperature is higher than for the colder months. The monthly median values for TA, TS and TD for the minimum duct height and the maximum duct height are shown in Figures 11 and 12, respectively. In these figures, the spreads between the TA and TS values indicate the differences in the stability between minimum and maximum seasons. The minimum season averages between slightly

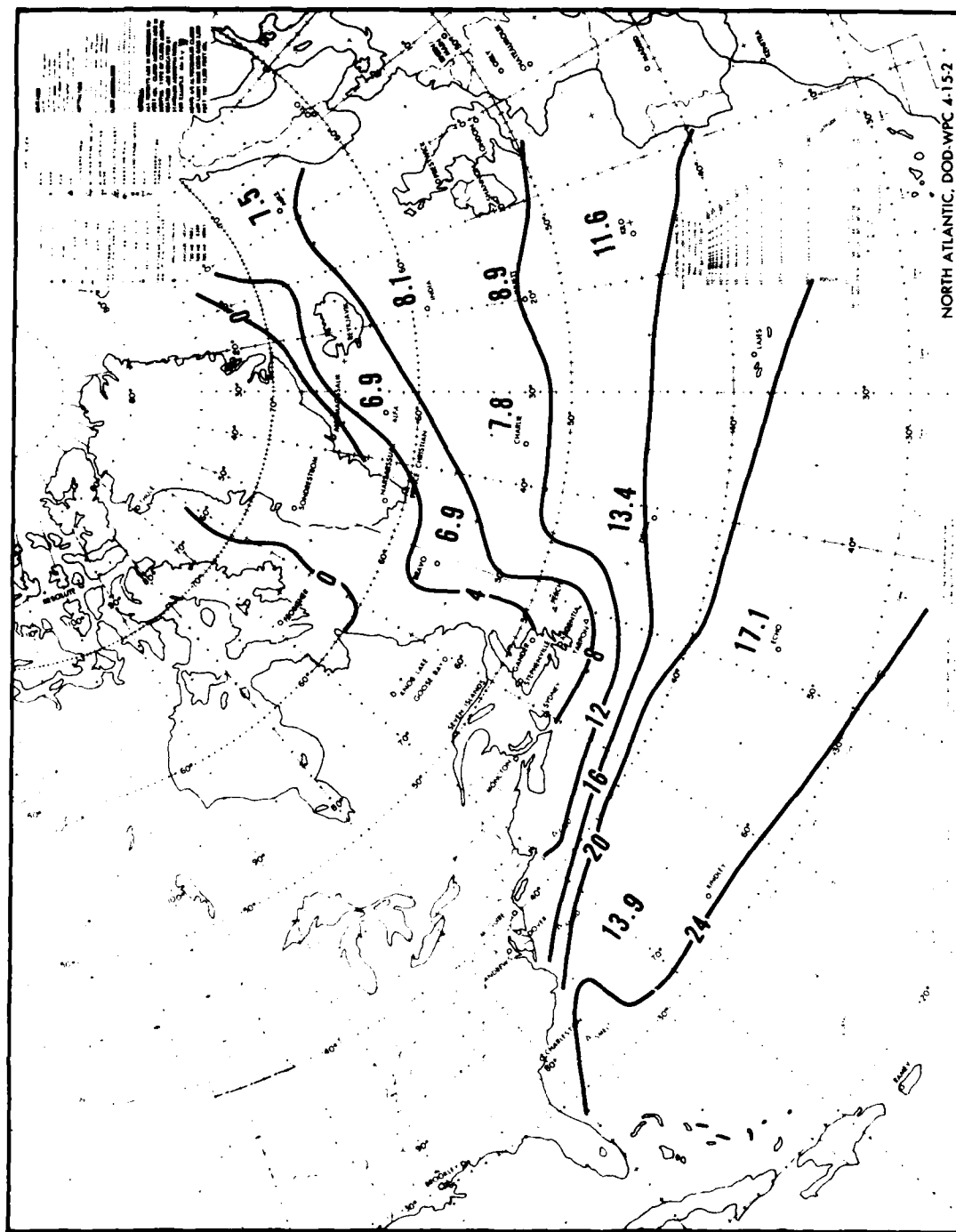


Figure 9. Sea surface temperature isopleths and maximum median duct heights for November (in meters, at each ocean weather station).

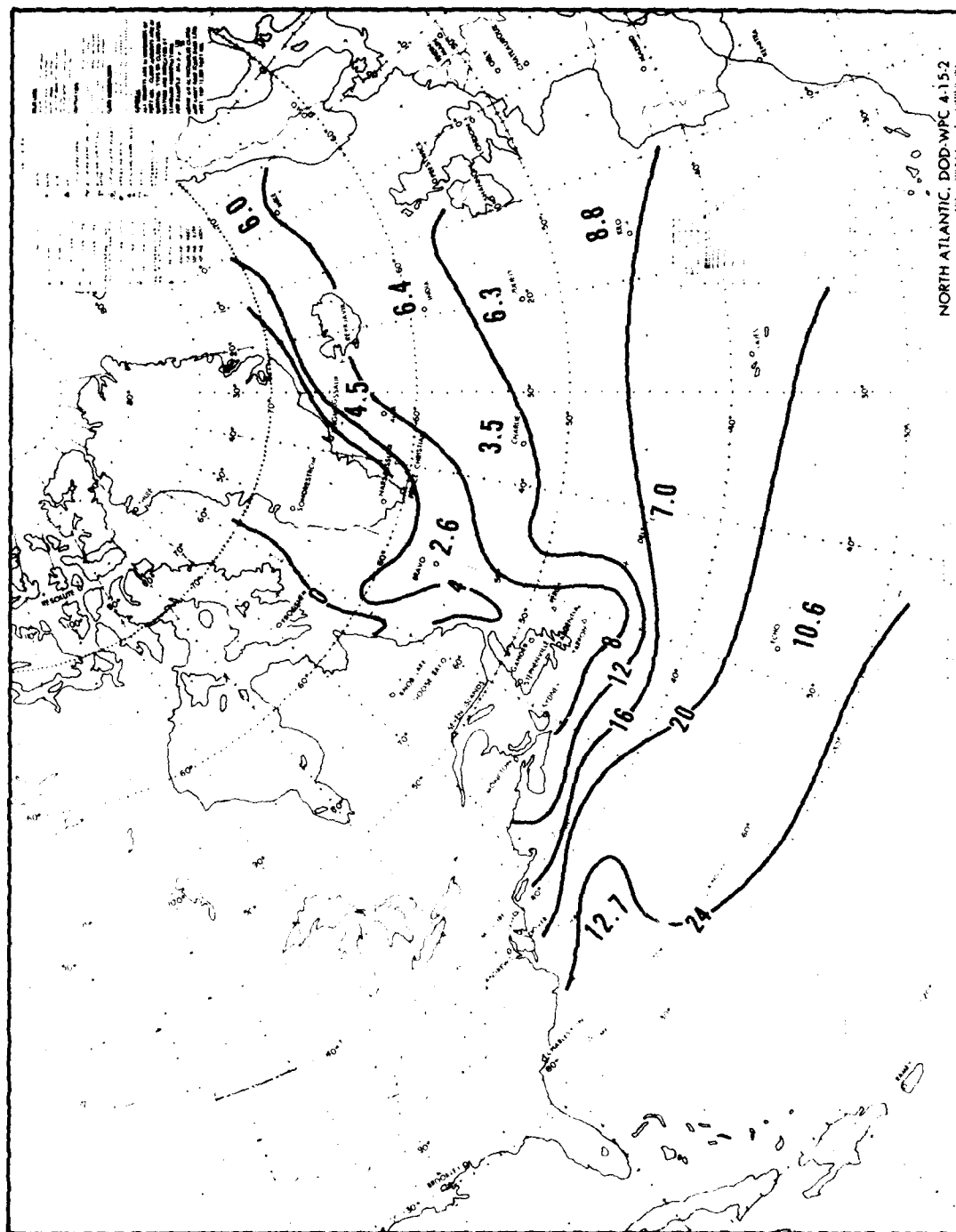


Figure 10. Sea surface temperature isopleths and maximum median duct heights for June (in meters, for each ocean weather station).

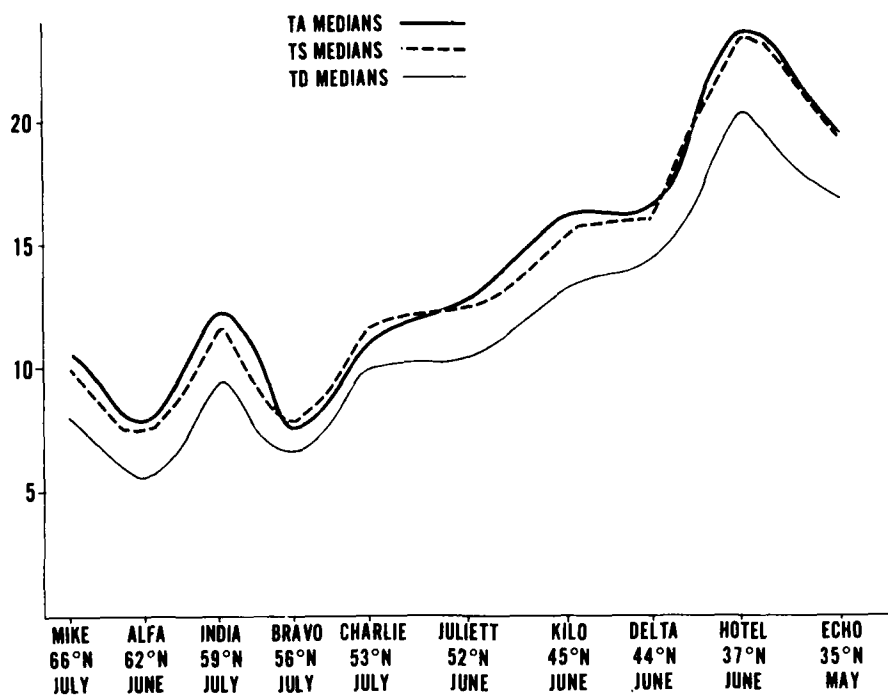


Figure 11. Median duct heights for the minimum-height season at each OWS.

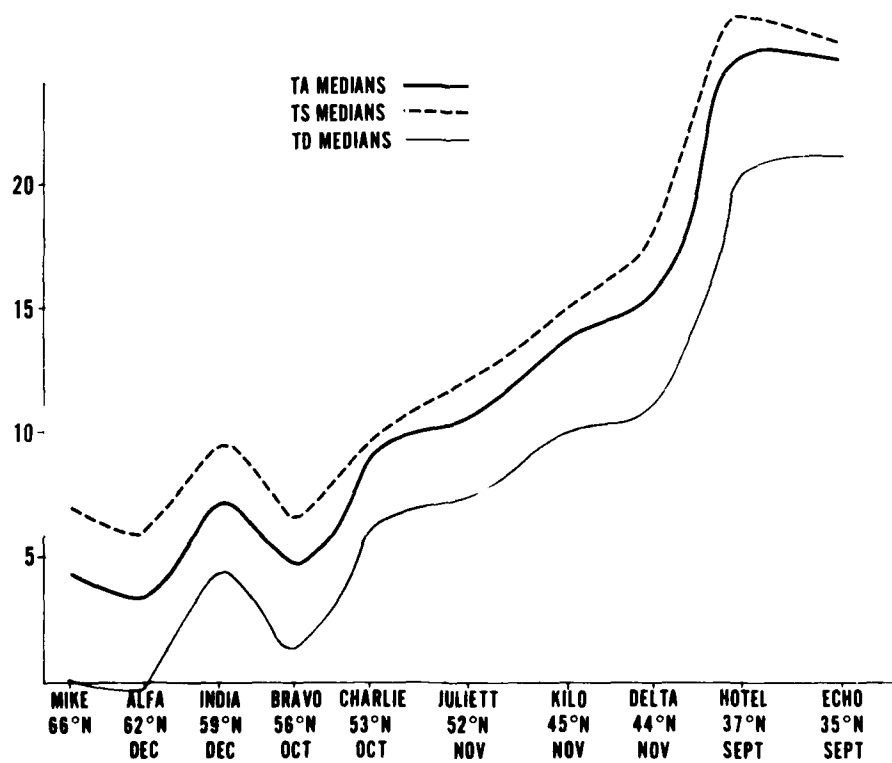


Figure 12. Median duct heights for the maximum-height season at each OWS.

stable to neutral. Also apparent in Figures 11 and 12 are the higher values of TD that occur during the minimum season. This one factor alone would cause lower duct heights due to the smaller values of ΔN .

Wind speed is also a factor in seasonal variations of duct height; in unstable conditions, duct height is proportional to wind. Table 2 summarizes the median wind values for each ocean weather station for the months of November and June. With only two exceptions, the month with the highest duct heights also has the highest median winds. The two exceptions are the two lowest-latitude stations, where winds are not as strong and have smaller seasonal variations. The overriding factor that causes the duct height seasonal variation at these two stations is apparently the variation in air temperature which causes change in the stability regime.

Table 2. Median values for wind, duct height, and TA-TS at 10 ocean weather stations in the North Atlantic.

OWS	LAT	Maximum Season (Nov)			Minimum Season (Jun)		
		Wind (Med.)	D (Med.)	(TA-TS) (Med.)	Wind (Med.)	D (Med.)	(TA-TS) (Med.)
ALFA	62	22.2	6.9	-2.6	14.0	4.5	0.2
BRAVO	56	21.6	6.9	-1.5	13.9	2.6	0.2
CHARLIE	53	21.2	7.8	-0.5	14.3	3.5	0.4
DELTA	44	21.4	13.4	-2.0	15.6	7.0	0.1
ECHO	35	12.2	16.3	-0.6	13.2	10.7	0.0
HOTEL	37	13.5	17.9	-1.7	12.9	12.7	0.3
INDIA	59	23.8	8.1	-2.1	15.3	6.4	0.7
JULIETT	52	21.9	8.9	-1.5	15.6	6.3	0.2
KILO	45	20.0	11.6	-1.1	13.7	8.0	0.6
MIKE	66	21.5	7.5	-2.5	13.2	6.0	0.5

The months with minimum duct heights are also months whose median stability is near neutral and slightly stable. Under stable condition $D \propto \frac{1}{U}$, higher winds would lead to lower duct heights. However, high surface winds are normally associated with unstable conditions, since that situation is needed to bring down to the surface the higher winds aloft. During lower wind conditions the stability borders on neutrality, and winds are not as much a factor.

6. SUMMARY

The occurrence of higher duct heights with lower latitudes results from the generally higher sea surface temperatures which, in turn, lead to higher air temperatures. Both of these trends lead to higher ducts.

The occurrence of greater duct heights during the late fall and early winter results from this season's greater instabilities, lower relative humidities and generally stronger winds. The minimum season (late spring and early summer) results from the combination of higher relative humidities, more nearly neutral stabilities and lower mean winds. However, care must be exercised for slightly stable conditions, with low winds and humidities, since these conditions (theoretically) can lead to higher ducts than under neutral or slightly unstable conditions.

In general, in mid-latitude regions, higher duct heights occur during the late fall and early winter, and at the lower latitudinal part of the regions.

REFERENCES

- Bean, B. R. and E. J. Dutton, 1967: Radio meteorology. NBS monograph 92. National Bureau of Standards, Washington, DC.
- Gossard, E. E., 1978: The height distribution of refractive index structure parameter in an atmosphere being modified by spatial transition at its lower boundary. Radio Sci., 13, 3, p. 489.
- Hitney, H. V., 1975: Propagation modeling in the evaporation duct. NELC TR-1947. Naval Electronics Laboratory Center, San Diego, CA 92152.
- Jeske, H., 1971. The state of radar range propagation over sea. Tropospheric radio wave propagation, part II. NATO-AGARD.
- Sweet, W. 1979: Monthly climatology for evaporation duct occurrence in the North Atlantic Ocean. NAVENVPREDRSCHFAC TR 79-01. Naval Environmental Prediction Research Facility, Monterey, CA 93940.
- Naval Avionics Facility Indianapolis (NAFI), 1977: Development plan for shipboard automatic weather station; app. J, modeling and uncertainty in the maritime evaporation duct. NAFI TR-2104. Naval Avionics Center, Indianapolis, IN 46218.
- Naval Ocean Systems Center (NOSC), 1978: Surface duct effects on fleet radars (U). NOSC TD-144, NAVOCEANSYSCEN, San Diego, CA 92152. (Report classified CONFIDENTIAL.)
- Naval Weather Service Command (NWSC), rev. 1974: U.S. Navy marine climatic atlas of the world, vol. 1, North Atlantic Ocean. Naval Air Systems Command 520-1C-528.

Distribution List

Commander in Chief
U.S. Atlantic Fleet
Norfolk, VA 23511

Commander in Chief
U.S. Pacific Fleet
Pearl Harbor, HI 96860

Commander in Chief
Attn: Meteorological Officer
U.S. Naval Forces, Europe
FPO New York 09510

Commander
Second Fleet
FPO New York 09501

Commander
Third Fleet
Pearl Harbor, HI 96860

Commander
Seventh Fleet (N30W)
Attn: Fleet Meteorologist
FPO San Francisco 96601

Commander
Sixth Fleet
FPO New York 09501

Commander
U.S. Naval Forces, Azores
APO New York 09406

Commander
U.S. Naval Forces, Caribbean
FPO Miami 34051

Commander
U.S. Naval Forces, Iceland
FPO New York 09571

Commander
Amphibious Group 2
Attn: Meteorological Officer
FPO New York 09501

Commander
Amphibious Group 1
Attn: Meteorological Officer
FPO San Francisco 96601

Commander
Surface Warfare Development Group
Naval Amphibious Base, Little Creek
Norfolk, VA 23521

Commander
Naval Surface Group, Mediterranean
Box 35
FPO New York 09521

Commanding Officer
USS AMERICA (CV-66)
Attn: Meteorological Officer
FPO New York 09531

Commanding Officer
USS FORRESTAL (CV-59)
Attn: Meteorological Officer
FPO Miami 34080

Commanding Officer
USS INDEPENDENCE (CV-62)
Attn: Meteorological Officer
FPO New York 09537

Commanding Officer
USS JOHN F. KENNEDY (CV-67)
Attn: Meteorological Officer
FPO New York 09538

Commanding Officer
USS NIMITZ (CVN-68)
Attn: Meteorological Officer
FPO New York 09542

Commanding Officer
USS DWIGHT D. EISENHOWER (CVN-69)
Attn: Meteorological Officer
FPO New York 09532

Commanding Officer
USS SARATOGA (CV-60)
Attn: Meteorological Officer
FPO New York 09587

Commanding Officer
USS CONSTELLATION (CV-64)
Attn: Meteorological Officer
FPO San Francisco 96635

Commanding Officer
USS CORAL SEA (CV-43)
Attn: Meteorological Officer
FPO San Francisco 96632

Commanding Officer
USS ENTERPRISE (CVN-65)
Attn: Meteorological Officer
FPO San Francisco 96636

Commanding Officer
USS KITTY HAWK (CV-63)
Attn: Meteorological Officer
FPO San Francisco 96634

Commanding Officer
USS MIDWAY (CV-41)
Attn: Meteorological Officer
FPO San Francisco 96631

Commanding Officer
USS RANGER (CV-61)
Attn: Meteorological Officer
FPO San Francisco 96633

Commanding Officer
USS MOUNT WHITNEY (LCC-20)
Attn: Meteorological Officer
FPO New York 09517

Commanding Officer
USS BLUE RIDGE (LCC-19)
Attn: Meteorological Officer
FPO San Francisco 96628

Commanding Officer
USS GUADALCANAL (LPH-7)
Attn: Meteorological Officer
FPO New York 09562

Commanding Officer
USS GUAM (LPH-9)
Attn: Meteorological Officer
FPO New York 09563

Commanding Officer
USS INCHON (LPH-12)
Attn: Meteorological Officer
FPO New York 09529

Commanding Officer
USS IWO JIMA (LPH-2)
Attn: Meteorological Officer
FPO New York 09561

Commanding Officer
USS NEW ORLEANS (LPH-11)
Attn: Meteorological Officer
FPO San Francisco 96627

Commanding Officer
USS OKINAWA (LPH-3)
Attn: Meteorological Officer
FPO San Francisco 96625

Commanding Officer
USS TRIPOLI (LPH-10)
Attn: Meteorological Officer
FPO San Francisco 96626

Commanding Officer
USS PUGET SOUND (AD-38)
Attn: Meteorological Officer
FPO New York 09544

Commanding Officer
USS LASALLE (AGF-3)
Attn: Meteorological Officer
FPO New York 09577

Naval Deputy to the Administrator
NOAA
Room 200, Page Bldg. #1
3300 Whitehaven St. NW
Washington, DC 20235

Officer in Charge
NAVOCEANCOMDET
Federal Bldg.
Asheville, NC 28801

Officer in Charge
NAVOCEANCOMDET
Naval Air Station
Brunswick, ME 04011

Officer in Charge
NAVOCEANCOMDET
Naval Air Station
Cecil Field, FL 32215

Officer in Charge
NAVOCEANCOMDET
Naval Station
Charleston, SC 29408

Officer in Charge
U.S. NAVOCEANCOMDET
Box 16
FPO New York 09593

Officer in Charge
NAVOCEANCOMDET
Box 9048
Naval Air Station
Key West, FL 33040

Officer in Charge
U.S. NAVOCEANCOMDET
Box 72
FPO New York 09510

Officer in Charge
U.S. NAVOCEANCOMDET
Naples, Box 23
FPO New York 09521

Officer in Charge
U.S. NAVOCEANCOMDET
U.S. Naval Station
FPO Miami 34051

Officer in Charge
U.S. NAVOCEANCOMDET
U.S. Naval Air Facility
FPO New York 09523

Officer in Charge
U.S. NAVOCEANCOMDET
FPO New York 09571

Commanding Officer
Naval Research Lab
Attn: Code 2620
Washington, DC 20390

Commanding Officer
Office of Naval Research
Eastern/Central Regional Office
Bldg. 114 Sect. D
666 Summer St.
Boston, MA 02210

Commanding Officer
Office of Naval Research
1030 E. Green Street
Pasadena, CA 91101

Commanding Officer
Naval Ocean Research & Dev. Activity
Code 101
NSTL Station
Bay St. Louis, MS 39529

Commander
NAVOCEANCOM
NSTL Station
Bay St. Louis, MS 39529

Commanding Officer
Fleet Numerical Oceanography Center
Monterey, CA 93940

Commanding Officer
Fleet Numerical Oceanography Center
Geophysics Tactical Readiness Lab
Monterey, CA 93940

Commanding Officer
Naval Western Oceanography Center
Box 113
Pearl Harbor, HI 96860

Commanding Officer
Naval Eastern Oceanography Center
McAdie Bldg. (U-117)
Naval Air Station
Norfolk, VA 23511

Commanding Officer
U.S. Naval Oceanography Command Center
Box 31
FPO New York 09540

Commanding Officer
U.S. Naval Oceanography Command Facility
FPO Seattle 98762

Superintendent
U.S. Naval Academy
Library Acquisitions
Annapolis, MD 21402

Commander
NAVAIRSYSCOM
Attn: Library (Air-954)
Washington, DC 20361

Commander
NAVAIRSYSCOM
Code Air-553)
Meteorological Systems Div.
Washington, DC 20360

Commander
NAVAIRSYSCOM
Code Air-370
Washington, DC 20361

Commander
NAVAIRSYSCOM
Attn: CAPT C.M. Rigsbee
Code Air-03
Washington, DC 20361

Commander
Naval Ocean Systems Center
Attn: Code 4473
San Diego, CA 92152

Commander
Earth & Planetary Sciences
Code 3918
Naval Weapons Center
China Lake, CA 93555

Commander
Naval Ship Rsch. & Dev. Center
Code 5220
Bethesda, MD 20084

Director
Navy Science Assistance Program
Naval Surface Weapons Center
White Oaks
Silver Spring, MD 20910

Naval Space Systems Activity
Code 60
P.O. Box 93960
Worldway Postal Center
Los Angeles, CA 90009

Commander
Pacific Missile Test Center
Attn: Geophysics Officer, Code 3250
Pt. Mugu, CA 93042

Weather Service Officer
Marine Corps Air Facility
Quantico, VA 22134

Commander
AWS/DN
Scott AFB, IL 62225

USAFETAC/TS
Scott AFB, IL 6225

3350th Technical Training Group
TTGU-W/STOP 623
Chanute AFB, IL 61868

Officer in Charge
Service School Command
Detachment Chanute/STOP 62
Chanute AFB, IL 61868

1st Weather Wing (DON)
Hickam AFB, HI 96853

AFOSR/NC
Bolling AFB
Washington, DC 20312

Engineer Topographic Labs
Attn: ETL-GS-A
Ft. Belvoir, VA 22060

Director
Defense Technical Information
Center
Cameron Station
Alexandria, VA 22314

Director
Office of Env. & Life Sciences
Office of the Undersecretary
of Defense for Rsch. & Eng.
Room 3D129
The Pentagon
Washington, DC 20301

Director
Technical Information
Defense Advanced Research
Projects Agency
1400 Wilson Blvd.
Arlington, VA 22209

Chief, Marine Science Section
U.S. Coast Guard Academy
New London, CT 06320

Commanding Officer
U.S. Coast Guard Oceanographic Unit
Bldg. 159-E
Washington Navy Yard
Washington, DC 20390

Acquisitions Section IRDB-D823
Library & Info. Serv. Div.
NOAA
6009 Executive Blvd.
Rockville, MD 20852

National Weather Service
Eastern Region
Attn: WFE3
585 Stewart Ave.
Garden City, NY 11530

NOAA Research Facilities Center
P.O. Box 520197
Miami, FL 33152

Chief, Operations Branch
Air Resources Lab, NOAA
P.O. Box 14985 AEC
Las Vegas, NV 89114

Director
Atlantic Oceanographic & Meteor. Labs.
15 Rickenbacker Causeway
Virginia Key
Miami, FL 33149

Director
Division of Atmospheric Sciences
National Science Foundation
Room 664
1800 G. Street, NW
Washington, DC 20550

Chairman
Department of Meteorology
Massachusetts Institute of Technology
Cambridge, MA 02139

Atmospheric Sciences Dept.
University of Washington
Seattle, WA 98195

Chairman
Department of Meteorology
University of Wisconsin
Meteorology & Space Science Bldg.
1225 West Dayton St.
Madison, WI 53706

Atmospheric Sciences Dept.
Oregon State University
Corvallis, OR 97331

Dean of the College of Science
Drexel Institute of Technology
Philadelphia, PA 19104

Chairman
Department of Meteorology
University of Oklahoma
Norman, OK 73069

Chairman
Department of Meteorology
University of Utah
Salt Lake City, UT 84112

Chairman
Dept. of Meteorology &
Physical Oceano.
Cook College, P.O. Box 231
Rutgers University
New Brunswick, NJ 08903

Director of Research
Institute for Storm Research
University of St. Thomas
3812 Montrose Blvd.
Houston, TX 77006

Chairman
Dept. of Meteorology
California State University
San Jose, CA 95192

Documents/Reports Section
Library
Scripps Institute of
Oceanography
La Jolla, CA 92037

R.S.M.A.S. Library
University of Miami
4600 Rickenbacker Causeway
Virginia Key
Miami, FL 33149

Director
Coastal Studies Institute
Louisiana State University
Clark Hall
Attn: O. Huh
Baton Rouge, LA 70803

Dept. of Atmos. Sciences Library
Colorado State University
Foothills Campus
Ft. Collins, CO 80523

Research Library
Center for Environment & Man, Inc.
275 Windsor St.
Hartford, CT 06120

Meteorology Research, Inc.
464 W. Woodbury Rd.
Altadena, CA 91001

Library
The Rand Corp.
1700 Main St.
Santa Monica, CA 90405

Aerospace Corporation
Attn: Meteorology Section
P.O. Box 93957
Los Angeles, CA 90009

Environmental Research &
Technology Inc.
696 Virginia Rd.
Concord, MA 01742

The Executive Director
American Meteorological Society
45 Beacon St.
Boston, MA 02108

American Met. Society
Meteorological & Geoastrophysical
Abstracts
P.O. Box 1736
Washington, DC 20013

World Meteorological Organization
ATS Division
Attn: N. Suzuki
CH-1211, Geneva 20, Switzerland

Chairman
Dept. of Meteorology
McGill University
805 Sherbrooke St. W.
Montreal, Quebec
Canada H3A 2K6

Library
Atmospheric Environment Service
4905 Dufferin St.
Downsview M3H 5T7, Ontario
Canada

Director of Meteorology &
Oceanography
National Defense Hdq.
Ottawa, Ontario
K1A 0K2
Canada

Metoc Centre
Maritime Forces Pacific Hdq.
Forces Mail Office
Victoria, British Columbia VOS-1B0
Canada

Defence Research Establishment
Pacific
Attn: Director-General
Forces Mail Office
Victoria, British Columbia
Canada VOS 1B0

Meteorological Office Library
London Rd.
Bracknell, Berkshire
RG 12 2SZ
England

Library
Finnish Meteorological Institute
Box 503
SF-00101 Helsinki 10
Finland

Library
Institute of Marine Research
Box 166
SF-00141 Helsinki 14
Finland

The Deputy Director General of
Meteorology
(Climatology & Geophysics)
India Meteorological Dept.
Pune 411-005
India

Professor M. Poreh
Israel Institute of Technology
Technician City, Haifa
Israel 32000

Istituto Universitario Navale
Facolta Di Scienze Nautiche
Istituto Di Meteorologia E Oceanografia
80133 Napoli - Via AMM
Acton, 38 Italy

Maritime Meteorology Division
Japan Meteorological Agency
Ote-Machi 1-3-4 Chiyoda-Ku
Tokyo, Japan

Instituto De Geofisica
U.N.A.M. Biblioteca
Torre De Ciencias, 3ER Piso
Ciudad Universitaria
Mexico 20, D.F.

Koninklijk Nederlands
Meteorologisch Instituut
Postbus 201
3730 AE Debilt
Netherlands

Physics Laboratory of the National
Defence Research Organization TNO
P.O. Box 96864
2509 JG
The Hague, Netherlands

Bureau Hydrografie Der Koninklijke
Marine
AFD MILOC/METEO
Badhuisweg 171
Den Haag, Netherlands

The Librarian
New Zealand Oceanographic Institute
P.O. Box 12-346
Wellington North, New Zealand

Library
University of Stockholm
Dept. of Meteorology
Arrhenius Laboratory
S-106 91 Stockholm, Sweden

Chief Atmospheric Sciences Div.
World Meteorological Organization
P.O. Box 5
Geneva 20, Switzerland

END

DATE

FILMED

12-180

DTIC

AD-A091 665

NAVAL ENVIRONMENTAL PREDICTION RESEARCH FACILITY MON--ETC F/G 4/2
METEOROLOGICAL FACTORS AFFECTING EVAPORATION DUCT HEIGHT CLIMAT--ETC(U)
JUL 80 W SWEET
NEPRF-TR-80-02

UNCLASSIFIED

ML

2 of 2

AD A
091665



EVAPORATION

EVAPORATION

END

DATE
FILMED

7-81

DTIC

SUPPLEMENT

INFORMATION



NAVAL ENVIRONMENTAL PREDICTION RESEARCH FAC
MONTEREY, CALIFORNIA 93940

NEPRF/1
5600
Ser: 1
22 May

From: Commanding Officer
To: Distribution

Subj: NAVENVPREDRSCHFAC Technical Reports; changes in

1. Subject reports in which pen and ink changes should be

- a. TR 79-01, June 1979: Monthly climatology for evaporation duct occurrence in the North Atlantic Ocean
- b. TR 79-02, July 1979: Summary of an EASTPAC refractive structure climatology
- c. TR 80-01, February 1980: Anomalous microwave propagation assessment in the lower troposphere using a bulk meteorological parameter
- AD-A091665-d. TR 80-02, July 1980: Meteorological factors affecting evaporation duct height climatologies
- e. TR 80-05, October 1980: Assessment/forecasting of microwave propagation in the troposphere using model

2. On DD Forms 1473 of all subject reports listed in Paragraph

Block 10 should read . . . PE62759N

Block 11 should read . . . Naval Ocean Systems Center
San Diego, CA 92152

Block 14 should read . . . Naval Material Command
Department of the Navy
Washington, DC 20360

3. On p. 5 of TR 80-05,

Eq. (1) should read

$$\Delta N = N_w(T_a) - N_w(T_d)$$

Eq. (2) should read

$$\Delta N = B \left[\frac{e(T_a)}{T_a^2} - \frac{e(T_d)}{T_d^2} \right] =$$

adding Δ in Eq. (1), and deleting repeated expression $-e$ in Eq. (2).

GUSTAVE GOLD
By direction